AD-A120 535 COHERENT TRANSIENT EFFECT STUDIES OF RYDBERG ATOMS(U) 1/1
ARIZONA UNIV TUCSON OPTICAL SCIENCES CENTER
R L SHOEMAKER ET AL. SEP 82 N00014-79-C-0488

UNCLASSIFIED F/G 20/5 NL

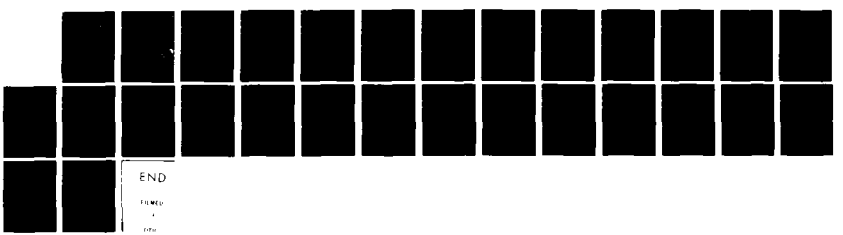

END

FILMED

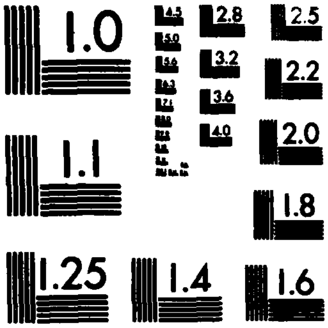

MICROCOPY RESOLUTION TEST CHART
NATIONAL BUREAU OF STANDARDS-1963-A

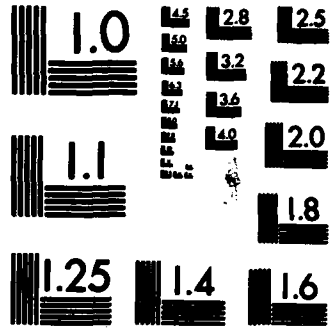

MICROCOPY RESOLUTION TEST CHART
NATIONAL BUREAU OF STANDARDS-1963-A

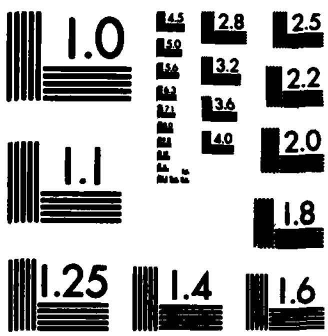

MICROCOPY RESOLUTION TEST CHART
NATIONAL BUREAU OF STANDARDS-1963-A

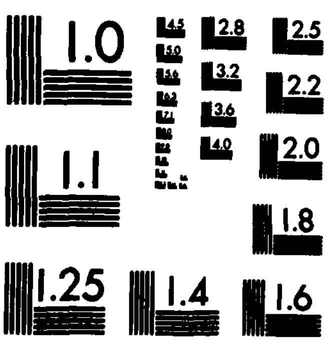

MICROCOPY RESOLUTION TEST CHART
NATIONAL BUREAU OF STANDARDS-1963-A

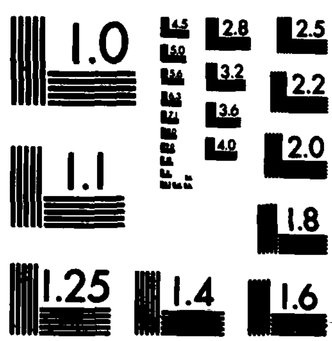

MICROCOPY RESOLUTION TEST CHART
NATIONAL BUREAU OF STANDARDS-1963-A

SECURITY CLASSIFICATION OF THIS PAGE (When Data Entered)

REPORT DOCUMENTATION PAGE

READ INSTRUCTIONS BEFORE COMPLETING FORM

1. REPORT NUMBER: N00014-79-C-0488-3 (12)	2. GOVT ACCESSION NO.: AD-A120535
3. RECIPIENT'S CATALOG NUMBER:	
4. TITLE (and Subtitle): "Coherent Transient Effect Studies of Rydberg Atoms"	5. TYPE OF REPORT & PERIOD COVERED: Final Rept
	6. PERFORMING ORG. REPORT NUMBER:
7. AUTHOR(s): Richard L. Shoemaker William H. Wing	8. CONTRACT OR GRANT NUMBER(s): N00014-79-C-0488
9. PERFORMING ORGANIZATION NAME AND ADDRESS: Physics Dept./Optical Sciences Center University of Arizona Tucson, AZ 85721	10. PROGRAM ELEMENT, PROJECT, TASK AREA & WORK UNIT NUMBERS: RR 011-03-01 NR 393-041
11. CONTROLLING OFFICE NAME AND ADDRESS: Office of Naval Research Dept. of the Navy Arlington, VA 22217	12. REPORT DATE: Sept. 1982 13. NUMBER OF PAGES: 26 pages
14. MONITORING AGENCY NAME & ADDRESS(if different from Controlling Office):	15. SECURITY CLASS. (of this report): Unclassified 15a. DECLASSIFICATION/DOWNGRADING SCHEDULE:

16. DISTRIBUTION STATEMENT (of this Report)

Unlimited distribution

17. DISTRIBUTION STATEMENT (of the abstract entered in Block 20, if different from Report)

DTIC ELECTE OCT 20 1982 D H

18. SUPPLEMENTARY NOTES

19. KEY WORDS (Continue on reverse side if necessary and identify by block number)

Coherent transient effects, Rydberg atoms, optical coherent transients, highly excited atoms.

20. ABSTRACT (Continue on reverse side if necessary and identify by block number)

New techniques for making time-resolved studies of atoms in highly excited (Rydberg) states were investigated. In particular, attempts were made to obse coherent transient effects produced via CO_2 laser irradiation, from a high density atomic Rydberg vapor produced by stepwise dye laser excitation, but no suc effects were observable. It was found that this result was due to a very rapid collisional decay process which occurs in a Rydberg gas at the densities requi for transient experiments ($\sim 10^{12}$ atoms/cm^3). The decay process was studied using ion collection and fluorescence techniques.

DD FORM 1 JAN 73 1473 EDITION OF 1 NOV 65 IS OBSOLETE S/N 0102-014-6601

82 10 20 039

SECURITY CLASSIFICATION OF THIS PAGE (When Data Ent

AD A120535

DTIC FILE COPY

Report N0014-79-C-0488-3

COHERENT TRANSIENT EFFECT STUDIES OF RYDBERG ATOMS

Richard L. Shoemaker
Optical Sciences Center
University of Arizona
Tucson, AZ 85721

William H. Wing
Physics Department and Optical Sciences Center
University of Arizona
Tucson, AZ 85721

September 1982
Final Report

Unlimited Distribution

Prepared for
OFFICE OF NAVAL RESEARCH
Department of the Navy
Arlington, VA 22217

I. Introduction

This research performed under this contract was concerned with the development of coherent transient techniques which could be applied to the study of highly excited (Rydberg) atoms. There has been a recent resurgence of interest in Rydberg atoms, and these time domain methods provide a powerful tool to investigate the properties of such atoms.

Coherent transient effects constitute a complex class of phenomena arising from the nonlinear interaction of radiation with matter.[1,2] Historically, they were first observed in the radiofrequency regime, in transient nuclear magnetic resonance (NMR) studies starting in the late 1940's. In the mid-1960's, after the development of lasers, coherent transient phenomena were observed in the optical regime. The phenomena in the optical and NMR regimes are closely related in the sense that the same fundamental equations, the Bloch equations, govern the time evolution of the system. Nevertheless, the difference of several orders of magnitude in the frequency means that the solutions of the Bloch equations sometimes are qualitatively different in the two regimes.

In general these transient effects arise when a sample is coherently excited by a sequence of resonant or near-resonant radiation pulses, and is manifested in the absorption or emission of radiation by the sample. The most widely known example of such a coherent transient effect is the photon echo and its NMR analog, the spin echo.[3] A photon echo arises when a sample is prepared by two suitable resonant light pulses, separated by a delay time T. At time $t = 2T$, the sample spontaneously emits a third pulse, the photon echo. The dependence of the echo amplitude on the delay time T is a sensitive measure of certain kinds of collisional processes. Specifically, the photon echo measures the effectiveness of collisions in destroying the off-diagonal density matrix element. There are many other lesser-known coherent transient phenomena, yielding specific information about the spectrum or collisional processes in the sample.

Coherent optical transient technology is a rather advanced art when applied to molecular gases. Many phenomena have been studied, including optical nutation,[4] optical free induced decay,[5] edge echoes,[5] photon echoes,[2,5] stimulated echoes,[2] Carr-Purcell echo trains,[7] modulated photon echoes,[8] delayed nutation[7] optical rotary saturation,[9] adiabatic rapid passage,[10] and coherent Raman beats.[11] In contrast, relatively few experiments have been performed on atomic systems[12]. A major reason for the relative paucity of experiments on atoms is that the lifetimes of the low-lying states of atoms, in which most atomic physics is done, is too short to be conveniently studied in the time domain. This experimental difficulty has deterred many researchers in the past from attempting to observe coherent transient phenomena in atoms.

However, in highly excited (Rydberg) states of atoms, the lifetimes are much longer than in lower excited states. Rydberg lifetimes can be microseconds or more, allowing sufficient time to perform a coherent transient experiment. Rydberg-to-Rydberg transitions lie in the microwave or infrared frequency regimes rather than in the visible. Although experiments with (visible) tunable dye lasers are therefore not possible, one can use powerful, stable cw infrared molecular lasers. The high density of states of the Rydberg manifold creates a large number of coincidences between atomic intervals and laser lines. Other characteristics such as the transition dipole matrix elements and the Stark effect coefficients are also very favorable. Thus atomic Rydberg states are very good candidates for coherent transient experiments.

There are excellent reasons for studying Rydberg atoms. Their properties are quite unlike those of the "ordinary" atoms conventionally studied.[13] Rydberg atoms are very large, potentially long-lived, and fragile. Their structure and behavior is relatively simple to model theoretically, allowing a close relationship between experiment and theory. Thus from a purely scientific point of view, these exotic atoms are quite interesting. Furthermore, detailed knowledge of Rydberg atom behavior may have practical applications. Some examples include: an understanding of collisional energy transfer and other aspects of plasmas, energy deposition in gases, the design and construction of atomic Rydberg lasers, the use of Rydberg atoms as high-sensitivity microwave detectors (already demonstrated by Figger et al),[14] and possible applications of Rydbergs as a charge exchange medium in the production of intense, very tightly focussed, neutral atomic beams for micromachining or integrated circuit fabrication.

The field of Rydberg atom interactions contains a large and growing number of contributions. However, nearly all experiments have been performed in the frequency domain, and relatively few in the time domain.[15-21] We hoped that our transient experiments would help to rectify this imbalance and complement the many frequency domain studies. As discussed in Section IV, this hope was not realized in the way we had anticipated.

II. Scientific Approach

The main thrust of the research was to study Rydberg atoms via coherent transient effects on transitions between two atomic Rydberg states. To do this, we utilized an excitation technique that selectively produces a population in one of the two Rydberg levels. Specifically, we used a pair of pulsed tunable dye lasers in a two-step excitation scheme. Figure 1 illustrates this for a specific transition in sodium vapor. Each dye laser was tuned to exact resonance with the atomic transition it was to pump, and the two dye laser outputs were synchronized in time by pumping them with beams split from a single pulsed nitrogen laser. In this way a large fraction of the initial ground state atom population are excited to any desired Rydberg level during the 5-nsec width of the dye laser pulses. Because many different atoms,

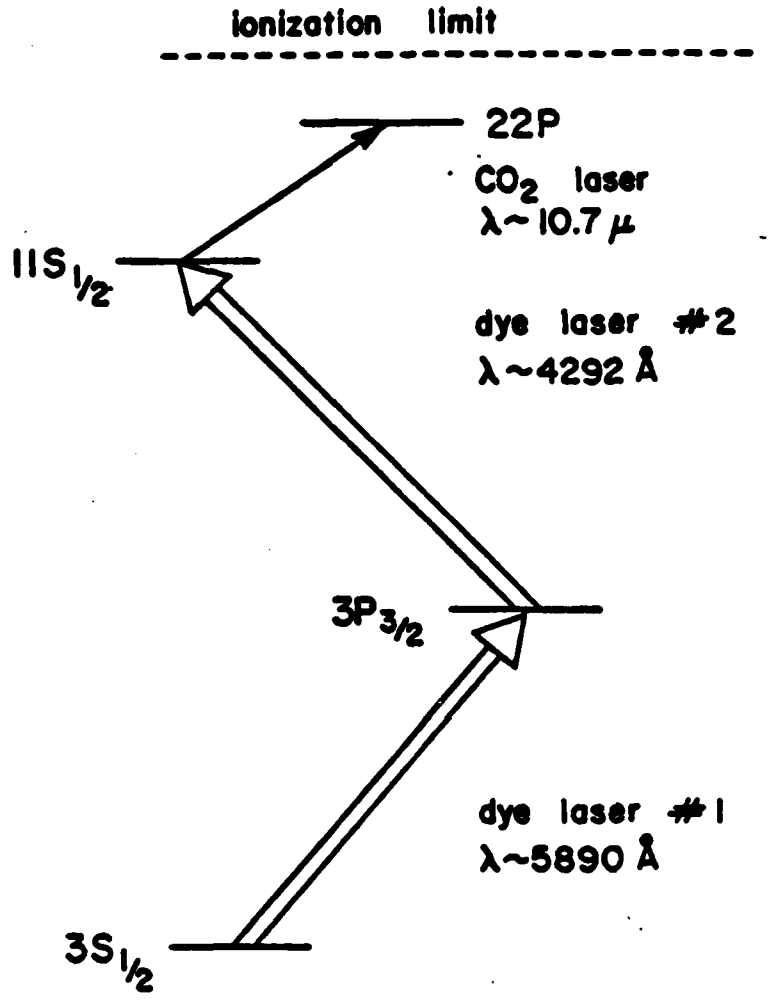

typical Rydberg coherent transient excitation scheme in Na vapor

Figure 1

particularly the alkali metals, have transitions from the ground and first excited state that fall within the tuning range of a dye laser, a large number of elements can be excited to Rydberg levels via two-step excitation. Furthermore, typical pulsed dye laser bandwidths and intensities are such that one can often saturate transitions with large oscillator strengths, thus ensuring a large population in the Rydberg level of interest.

Once a population of Rydberg atoms had been obtained, we needed to find a way to perform the coherent transient experiment before the atoms decay back down to lower levels. This was done using a cw CO_2 laser and Stark switching.[6] The idea behind this technique is the following: Instead of using a pulsed laser, suppose a cw CO_2 laser is resonant with some transition between two Rydberg levels. Also, let the atoms be in a sample cell such that a pulsed electric field can be applied across the cell. Since the Rydberg transition is Doppler-broadened at the low ($<10^{-3}$ Torr) pressures used, only those atoms whose velocity is such that they are Doppler-shifted into resonance will be excited by the CO_2 laser. When the electric field is suddenly applied across the cell, the transition frequency is shifted owing to the difference in Stark coefficients for the upper and lower levels. This causes some new velocity group of atoms to suddenly be shifted into resonance and start to interact with the laser. If the electric field is then suddenly removed, this velocity group is shifted back out of resonance, and as far as the atoms are concerned, has effectively seen a pulse of radiation. Hence by simply turning on and off an electric field, we can apply any sequence of pulses we desire to a velocity group of atoms. If the transmitted laser beam is monitored with a detector, one can observe the transient effects produced in this group by the pulse train. The use of Stark switching to observe coherent transients has many advantages. These include: (1) the pulses are generated electronically, which allows any pulse train to be easily produced with nearly ideal pulse shapes; (2) the CO_2 laser itself produces only a dc signal, so the only ac signals present at the detector are just the transient effects one wants to observe; (3) the laser is cw, so its intensity and beam profile are stable and easily measured; (4) in experiments such as the photon echo, where the light is emitted in the forward direction, the atomic emission is shifted from the laser frequency and beats with the laser at the detector to give very sensitive heterodyne detection; (5) the high sensitivity allows optically thin samples to be used and thereby permits a simple theoretical interpretation of the experimental results. The Stark switching technique has been very successful in molecules, and, since one of us (RLS) was a coinventor of the technique,[6] we have had extensive experience with it at the University of Arizona.

In the Rydberg atom experiments, a further advantage of Stark switching was that a coherent transient experiment could easily be synchronized to start just after the population of Rydbergs is created by the dye lasers. The two dye laser beams and the cw CO_2 laser beam are

spatially superimposed and pass through a sample cell containing a pair of Stark plates. On receiving a trigger signal from the N_2 pump laser, a pulse generator applies a pulsed electric field across the cell. An infrared detector behind the cell then monitors the transmitted CO_2 beam plus any atomic emission signals (i.e., the coherent transient effects). The detector output is digitized to 8 bit accuracy at 2000 time points by a transient recorder and then sent to a microcomputer where repeated experiments can be scaled and signal averaged if desired. This method of data acquisition allows us to eliminate the undesirable effects of pulse-to-pulse amplitude fluctuations in the dye laser outputs.

For the experiments just described to be successful, the Rydberg transitions must satisfy a number of constraints. For example, we needed to have frequency matches between Rydberg transitions and CO_2 laser lines. These transitions should have large Stark effects and large transition dipole matrix elements. We also had to create Rydbergs in sufficient numbers to allow detection of the infrared transients. Finally, the Rydberg lifetimes needed to be on the order of a microsecond or more at the working density, when the probable size of collision cross sections and the effects of black body radiation are taken into account.

III. Description of the Experimental Apparatus

The observation of coherent transient effects between two Rydberg states is a complex experiment. Simultaneous operation of four lasers is required, along with a large amount of electronics, optics, and test equipment. In the paragraphs below, a description is given of how the various components were constructed along with discussions of the tests made to determine their proper operation.

Lasers

Four lasers were used in our experiments: a nitrogen pump laser, two independently tunable dye lasers, and a cw carbon dioxide laser. Only the nitrogen laser was purchased; the other three lasers were constructed in our laboratories.

The nitrogen laser was made by NRG and was originally supposed to provide 700 kW peak power in a 5 nsec pulse. However, the thyratron failed and had to be replaced by a spark gap (the thyratron is no longer manufactured), and the capacitor plates had to be replaced and modified. Currently we are able to obtain about 250 kW from this laser.

The two dye lasers and their associated dye circulation systems were constructed specifically for this experiment. They utilize the recently developed Littmann-Metcalf type of design which has a grazing incidence grating for frequency selection in a folded three-mirror cavity (see Fig. 2).[22] This design allows a very compact cavity and thus is well suited to short pulse N_2 lasers like the NRG. Our lasers were designed to be very stable and rigid, and they utilize flexure pivot bearings to provide stick-slip free tuning. We have been very pleased with their performance in this regard. The laser can easily be tuned to the peak of an atomic resonance and will remain there without adjustment for hours.

We acquired, built, or already had available a variety of diagnostic tools to monitor the laser performance. These include a very fast photodiode to measure the dye laser pulse lengths, a Scientech power meter with volume absorbing head for laser power measurements, two home-built 30 GHz Fabry-Perot etalons (one for 500 to 600 nm, one for 400 to 500 nm) to measure laser bandwidths, and a 0.25 meter monochromator for wavelength measurements. These diagnostics are essential as proper alignment of the lasers is rather tricky. In particular, we find that one cannot simply adjust for maximum power, as this gives a very broad spectral bandwidth for the laser output. Instead, one must maximize spectral brightness, i.e. power/bandwidth. When this is done we find that each laser provides 1 to 2 kW peak power with a bandwidth of ~8 GHz in a 5 nsec pulse. Since half of the N_2 laser output pumps each dye laser, the efficiency is somewhat over 1%. According to Littman, this is about what one expects for this type of laser when pumped by N_2.

The CO_2 laser used is a 1.5 meter ultrastable device, patterned after the design of Freed.[23] This laser was partially rebuilt and realigned for the Rydberg experiments. It

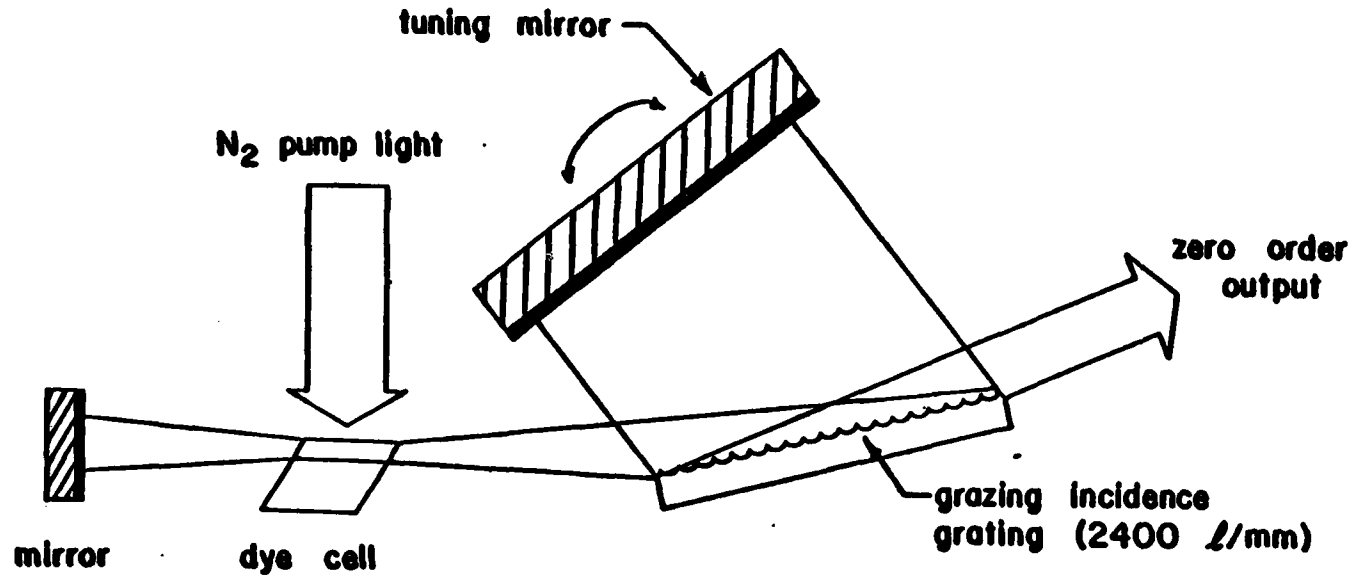

Littmann – style grazing incidence pulsed dye laser

Figure 2

provides 1 or 2 W of single mode TEM_{00} power on any of over 70 lines in the 9 and 10 μm bands of CO_2. Short-term frequency jitter is less than 50 kHz and long-term drift is about 2MHz/hr. Even better long-term stability can be obtained by locking the laser to line center. The laser is sealed off, and we have two discharge tubes: one for $^{12}CO_2$ and one for $^{13}CO_2$. Thus over 140 discrete frequencies are available. It is essential to know the molecular line on which the laser is oscillating. To do this we built into the system a 0.25 meter infrared monochromator which was calibrated using a HeNe laser and checked by observing several CO_2 laser - molecular transition overlaps in a Stark cell.

Optics and Sample Cell

The optical layout for the experiment is shown in Fig. 3. The two dye lasers were simultaneously pumped by the N_2 laser at 30 Hz. The dye laser pulses then stepwise excite a population of Rydberg atoms, and the cw CO_2 laser induces transitions between two Rydberg states. The second dye laser pulse is delayed about 6 nsec with respect to the first by means of an optical delay line in order to obtain maximum excitation. The two dye beams are then combined spatially and reflected off a germanium plate into the sample cell. The CO_2 laser beam was sent into the cell by transmission through the germanium plate.

The sample cell is a crucial component of the experiment, and its design is nontrivial since it must simultaneously meet many requirements. After trying and modifying several different models, we settled on the cell that is shown schematically in Figs. 4 and 5. It is a double window design, with an inner pair of hot windows and an outer pair of cold windows. The central section of the cell is heated and contains the alkali metal sample to be studied. The sections between the inner and outer windows are evacuated. The seal between the central section and the evacuated regions is the most difficult part of the design. The windows must pass both 10 μm infrared and visible light, and be resistant to attack by the hot alkali metal atoms. Alkali halide windows such as NaCl are the best choice in this situation. However, making a vacuum-tight seal between NaCl and another material that will remain leak-free during repeated temperature cyclings between 20°C and 300°C is extremely difficult. We chose not to attempt this. Instead, the inner windows were held against a lip in copper pistons by small clips and the copper pistons were held by spring tension against the ends of the central section of glass tubing. The resulting seal allows only minute amounts of alkali to escape into the evacuated region where it condenses on the cold walls. The copper plungers themselves are heated so no alkali condenses on them. The outer, cold windows are shielded from the small amounts of escaping alkali by lengths of 1-in. copper tubing attached to the cold end plates. This tubing also holds the springs which press the copper pistons against the central section of the cell.

The central portion of the cell is surrounded by magnetic shielding over which is wrapped heating tape and 2 in. of fiberglass insulation. Thermocouples under the shielding

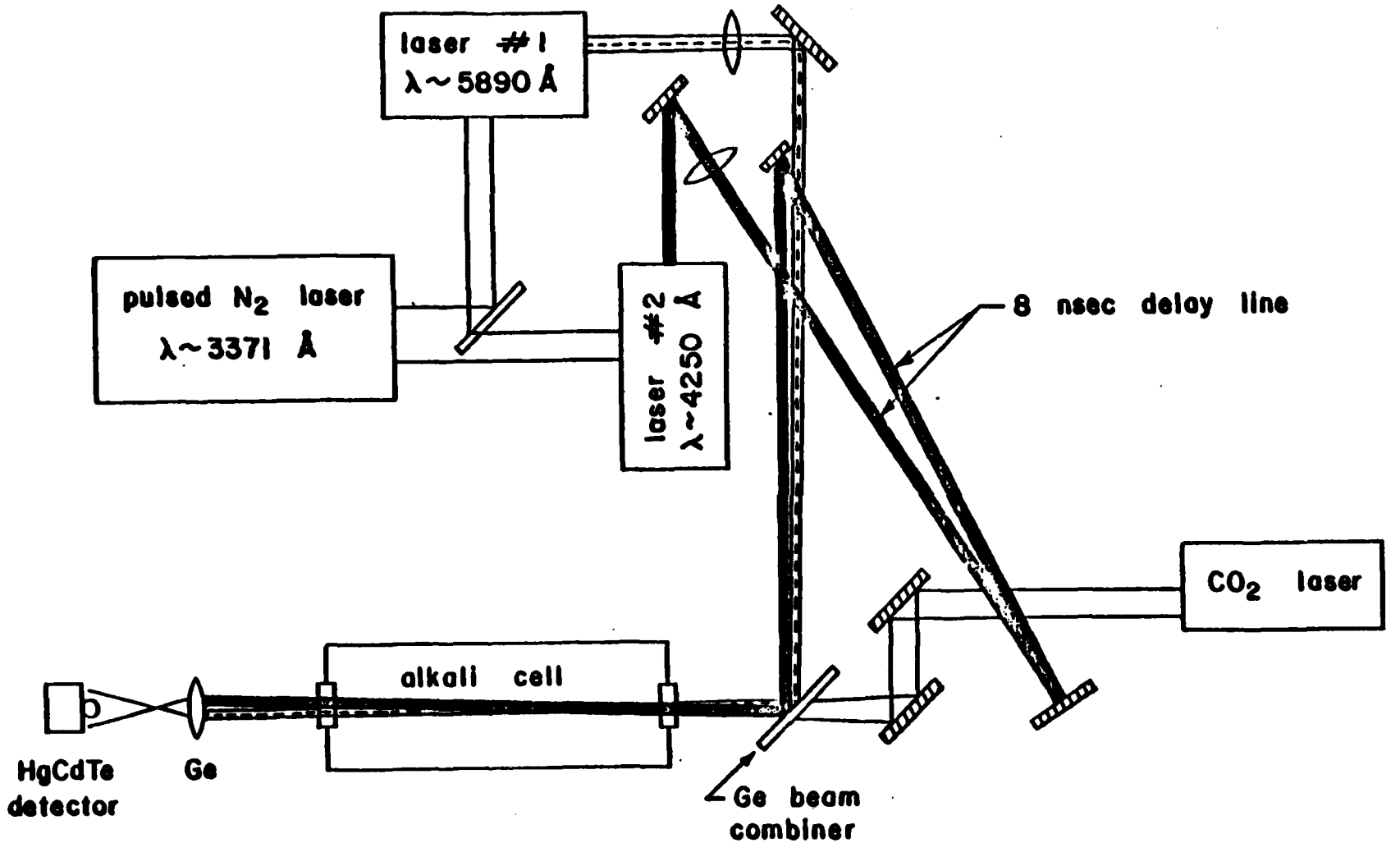

optical layout for coherent transient studies

Figure 3

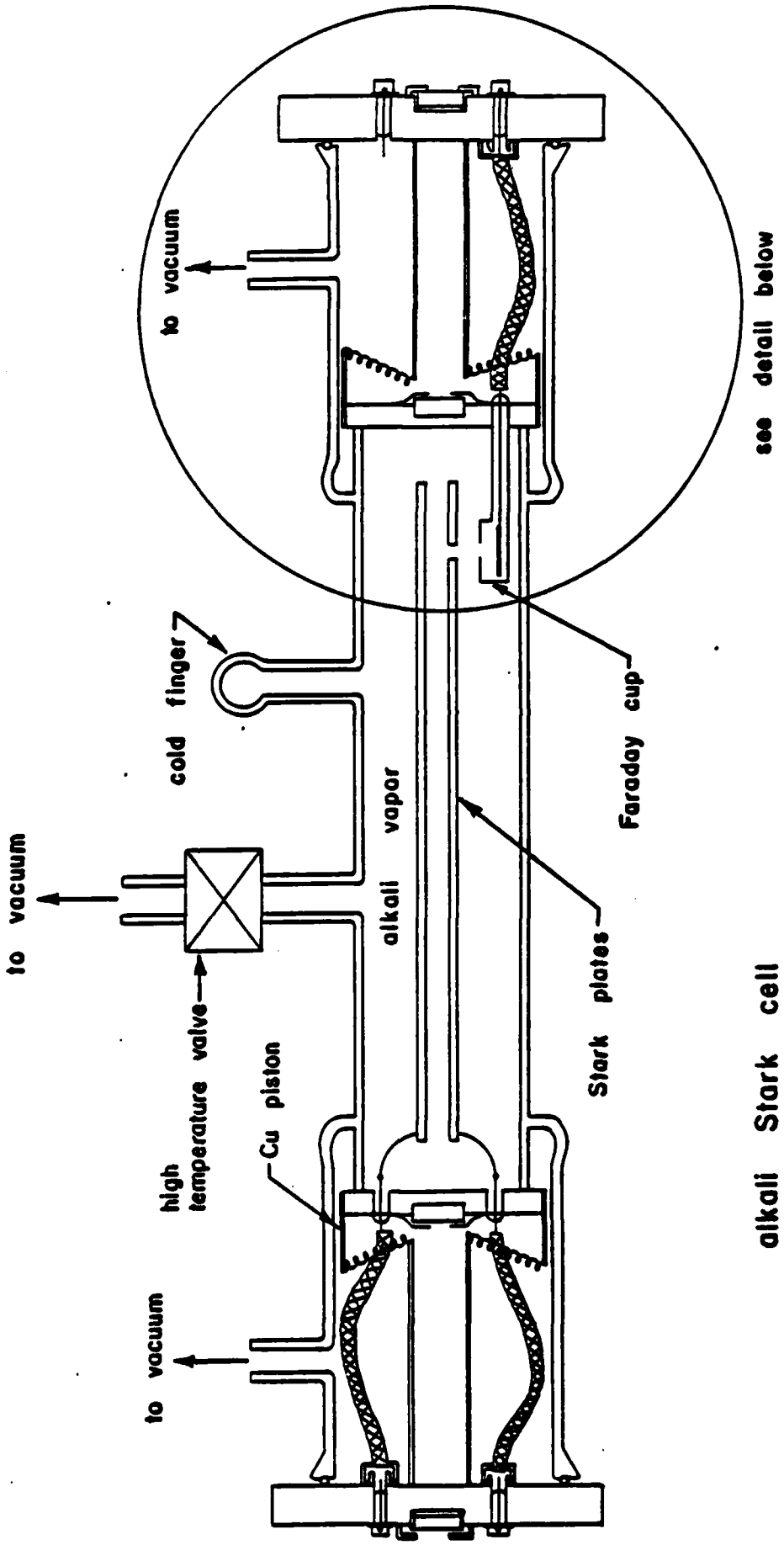
to vacuum
see detail below
cold finger
Faraday cup
to vacuum
alkali vapor
Stark plates
high temperature valve
Cu piston
to vacuum
alkali Stark cell
(heating mantle removed)

Figure 4

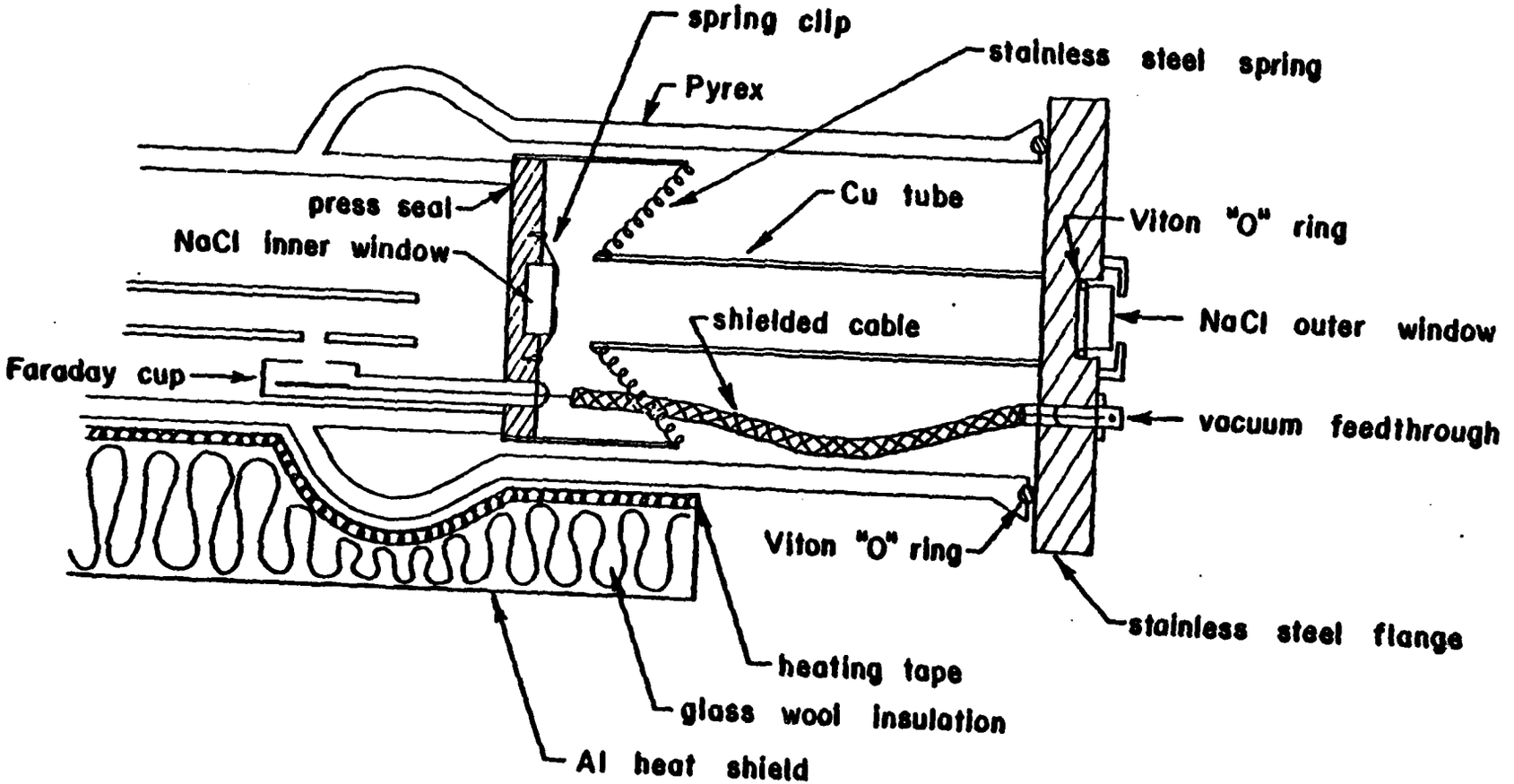

detail of alkali Stark cell

Figure 5

sense the temperature and provide feedback to a servo system which controls the heating tape. This system is equipped with a fail-safe breaker which prevents runaway heating should the thermocouples fail. There are two independent heating systems; one on the central cell section, and one on a small "cold finger" attached to the cell. The "cold finger" is maintained at a temperature about 20^{o} to 30^{o}C colder than the cell so that it determines the alkali metal vapor pressure and no condensation of alkali occurs in the cell itself.

A vacuum system was also constructed was also constructed for the experiments consisting of a vacuum manifold, cold trap, diffusion pump, and mechanical forepump, together with ion gauge and thermocouple gauge monitors. This system allowed us to evacuate the sample cell and fill it with pure alkali metal samples.

Inside the central cell section is a pair of Stark field plates. These are made from two 2 in. by 12 in. pieces of aluminized float glass, separated by precision 1/4 in. sapphire balls, and held in place by a set of glass supports. Electrical connection to the plates was made using vacuum feed-throughs in the copper plungers and end plates, and a special shielded cable which we have constructed, possessing a center conductor made of stainless steel rather than copper, in order to minimize the heat transfer. The center conductor is separated from copper braid shielding by ceramic spacers.

In addition to the Stark plates, an ion detection system was built into the cell. A tiny 1 mm wide by 10 mm long slot is cut in one of the Stark plates and a shielded Faraday cup is positioned behind the slot. By applying a voltage to the Stark plates, ions or electrons can be accelerated through the slot and detected by the charge collected in the Faraday cup circuit.

One of the Stark plates is connected to an adjustable dc bias voltage, while the other is connected to a custom-built pulse generator. This generator is triggered by a detector which monitors the N_2 laser and sends a pulse sequence to the Stark plates after an adjustable delay. The pulse lengths and amplitudes are also adjustable.

Detection Systems

A fast HgCdTe photodiode that monitors the CO_2 beam transmitted through the cell along with any emission from the Rydberg atoms, was used for the attempts to observe coherent transient effects. The detector output was amplified by a wideband preamp we built, containing a TIEF-151 transimpedance amplifier. The preamp output was then fed directly to a scope for visual observation or to a Biomation 8100 transient recorder for digitization. The Biomation is interfaced to a Z80-based microcomputer system which was constructed for this experiment. It has 48 kbytes of memory, an 8 in. floppy disk drive, two serial ports, four parallel ports, and two 12-bit D/A converters. The computer takes the data from the transient recorder and stores it in memory so that signal averaging,

background subtraction, and data analysis can be conveniently done.

A fluorescence monitoring system was also constructed to monitor the Rydberg population produced by the dye lasers. After trying several schemes for Rydberg detection, we found that the following works best for the n = 8 to 14 states in sodium that we were interested in: one monitors the ultraviolet fluorescence from the 4P → 3s transition at 3303 Å with a photomultiplier preceded by a filter to block visible radiation. The 4P state is populated by atoms which cascade down from the Rydberg state of interest, and the signals from the photomultiplier can be observed directly on an oscilloscope. Two other small cells were also built for resonance detection. One is simply a small fluorescence cell which can be operated independently of the sample cell. The other is a cell containing a thermionic diode of the type described by Stoicheff.[24] This is useful primarily for monitoring resonances involving higher Rydberg levels than those for which the fluorescence monitor is suitable.

In addition to the equipment, a number of calculations were also needed so that we would know where to look, what kinds of laser powers and bias voltages would be needed, etc.

Theoretical Calculations

It was essential for us to know which CO_2 lines and Rydberg transitions to look for. This is a nontrivial problem because there are hundreds of possible CO_2 laser lines, and equally many candidates for Rydberg transitions. Furthermore, the Rydberg transition frequencies are not known to the accuracy we would like. We developed a set of computer programs to tackle these problems. First of all, a program was written to calculate Rydberg energy levels. The program uses the very successful quantum defect formulation for the binding energy E, namely

$$E(n,L,J) = -\frac{R}{[n-\Delta(n,L,J)]^2}$$

where the quantum defect Δ is given by

$$\Delta(n,L,J) = \Delta_0(L,J) + \frac{\Delta_1(L,J)}{[n-\Delta_0(L,J)]^2} + \frac{\Delta_2(L,J)}{[n-\Delta_0(L,J)]^4}$$

and R is the Rydberg constant.[25] The Δ_i's include the effects of reduced mass and fine structure, and were determined by a least squares fit to the experimental energies given in the Bashkin and Stoner tables.[26]

A second program to calculate CO_2 laser frequencies was also written using the standard expansion in powers of J(J+1) with coefficients determined by Freed et al.[27] Next, a set of programs was written that calculates allowed transition frequencies using the Rydberg energy levels, sorts them in order of increasing frequency, and then looks for and

prints out any near coincidences between CO_2 laser lines and Rydberg transitions. The final thing we needed to know is the sign and approximate magnitude of the Stark effects in transitions which are nearly resonant. To do this, programs were first developed that calculate matrix elements, transition probabilities, and branching ratios for any desired atomic levels using the Coulomb approximation with quantum defects. These results are then used to calculate Stark shifts for any level. We can easily calculate the electric fields necessary to tune the atoms into coincidence with the laser radiation. We found that, due to the enormous Stark effects in Rydberg atoms, small fields of 30V or less are typically sufficient to shift resonances by as much as 1 to 2 GHz. In addition, these programs provide us with radiative lifetimes and dipole matrix elements. We found that the levels of interest have radiative lifetimes on the order of a microsecond or greater and that the dipole matrix elements for the Rydberg-Rydberg transitions are large, on the order of 0.1 - 1 Debye.

A potential complication in our experiments is the effect of blackbody radiation (BBR) on the Rydberg atoms. Although its influence is generally neglected in atomic physics, BBR can have effects on Rydberg atoms which are appreciable under some circumstances. The BBR drives electric dipole transitions among Rydberg states, redistributing the populations and shortening the lifetimes. We have performed[28] accurate calculations of BBR effects for realistic atoms, and find that even after BBR effects are taken into account the lifetimes still remain on the order of a microsecond or more.

IV. Summary of Research Results

The design and construction of the apparatus occupied us during the first year of the grant. When all the key pieces of equipment were operational, we did a series of tests to demonstrate proper operation of various aspects of the experiment. These test results may be summarized as follows:

1. The presence of sodium atoms in the desired Rydberg state was demonstrated by the appearance of a strong fluorescence signal (4P → 3S at 3303 Å) when both lasers were tuned to the appropriate wavelength, as measured on a calibrated monochromator. This signal disappears if either laser is detuned from resonance or if the beams are not spatially overlapped. By leaving the first laser resonant with the $3S_{1/2} \rightarrow 3P_{3/2}$ transition and varying the second laser frequency from 442 nm to 415 nm, we were able to populate any Rydberg state from 9S to 17S and 8D to 17D. Based on the collection geometry and measured fluorescence signals, the Rydberg density was estimated to be $>10^{11}$ atoms/cm^3. This density should be sufficient to see transient signals. By moving the photomultiplier back and forth along the length of the cell, we could also show that Rydbergs were being formed over the entire length of the cell.

2. By chopping the CO_2 beam, we verified that the beam was being detected by the HgCdTe detector. The CO_2 laser transition being used was determined by a calibrated monochromator which was checked against several known CO_2 laser - molecular transition overlaps. Finally, we verified that the CO_2 beam spatially overlapped the dye laser beams by inserting thermofax paper into the beam and noting where the dark spot is that the CO_2 beam produces in relation to the dye beams.

3. Operation of the Stark plates was demonstrated by observing that the fluorescence signal from the 3S - 11D stepwise excitation can be made to disappear by applying a sufficient voltage to the Stark plates. The transition is shifted out of resonance by the electric field at a voltage that roughly agrees with calculated values for the Stark shift of the 11D level.

4. When both dye lasers were resonant, we observed very interesting signals from the Faraday cup detector. These signals verified the proper operation of the ion detection system and also proved again the presence of substantial numbers of Rydbergs and the proper operation of the Stark plates. What we observed was a signal corresponding to ~ 10^{10} ions/cm^3 which appears when the dye pulses pass through the medium. The signal appeared as an ion pulse when the lower Stark plate was slightly negatively biased, and as an electron pulse when the plate was slightly positively biased. Also, it appeared only when both dye lasers were resonant. We comment at length on this signal below.

Following these preliminary tests, we started running the full experiment, searching for transient signals. After a period of unsuccessful searches, we discovered two problems in

the program that predicts frequency matches: a mistake in the CO_2 line labelling, and inaccurate values for the sodium line positions used to calculate quantum defects. These errors were corrected, and search experiments were begun again.

After a second long period of unsuccessful searches, we were forced to conclude that something else was wrong with the experiment. Being unable to find any problems with the apparatus, we began to look more closely for physics problems that may have been previously overlooked.

The first effect to be considered was superradiance. It is well known that superradiant emmission in the far infrared can occur when thin pencil-shaped volumes of Rydberg atoms are created.[29] The threshold condition for this process is given by

$$N > 8\pi/(\gamma_{ab}\, T_2^{*}\, L\, \lambda^2)$$

where N is the Rydberg atom density, L is the length of the sample, γ_{ab} is the homogeneous width of the superradiant transition and λ its wavelength. T_2^{*} is the Doppler dephasing time for the transition. On putting in numbers for our experimental conditions, we found that we were operating at densities very near or slightly above threshold.

Despite this result, there are two reasons why we feel that superradiance is not the primary cause of our failure to observe coherent transients. First of all, people who have worked with superradiance in Rydbergs claim that it is seldom possible to lose more than 50% of the Rydbergs when a superradiant pulse occurs. This should still have left us enough Rydbergs to see transients. Second, we did a series of experiments in which the dye laser beam diameters were expanded by a factor of 5 and the Na vapor pressure was reduced accordingly. These conditions should have brought us below the superradiant threshold and allowed transients to occur. None were observable, however.

The second effect to be considered was collisional ionization of the Rydberg atoms. We had noted earlier that an ion or electron pulse was observable when we monitored the voltage across the Stark plates after Rydbergs were created. The concern here is that an avalanching process might occur in which the Rydberg atoms are ionized either by collisions with other Rydbergs, with ground state atoms, or with electrons on ions produced by previous collisions. There is little experimental data regarding these processes in Rydbergs because almost all Rydberg experiments have been done in atomic beams where the atomic density is orders of magnitude lower than in our experiments. A notable exception is recent work by Haroche and his colleagues in which the spectrum of a very intense ($\sim 10^{15}$ atoms/cm^3) supersonic cesium beam was observed.[30] They found that the spectrum at these densities broadened into a near continuum, indicating the presence of a very fast decay process. They also observed, as we did, large numbers of ions being produced after the excitation pulse.

Haroche's results, plus our own experiments, convinced us that the collisional processes mentioned above were destroying the Rydbergs before a coherent transient experiment could be done (we need lifetimes of ~ 200 nsec. or greater in order to initiate the Stark pulse sequence and observe the response). We tried experiments with 5X expanded dye laser beams and correspondingly lower Rydberg densities but were still unable to observe transients. Going to much lower densities and much larger beam diameters (to keep the total number of absorbing atoms constant) might allow the observation of transients, but we were not able to try this as it would have required us to completely redesign and rebuild the sample cell, to buy beam expanding telescopes for the visible and infrared beams, and to re-do much of the optics.

Instead, we decided to try some investigations of the collisional decay by other techniques with the hope of determining in more detail what kinds of processes were occurring. We had two signals available to monitor the collisional decay: The ion or electron pulse appearing on the Stark plates or the Faraday cup, and the UV fluorescence signal from the 4p level in Na. Using our Biomation transient Digitizer, both signals were time-resolved and captured simultaneously. Because of the complex shape of the time-resolved signals and the large shot-to-shot variations between laser pulses, we eventually decided to monitor only the integrals of ion and fluorescence signals (integration was done digitally by the computer using the time resolved signals as inputs). In the remainder of this section we describe how this data was analyzed.

It is convenient to assign all of the sodium atoms in the cell into one of two different categories at the instant of cessation of the laser pulses. The first category consists of ground state sodium atoms, plus perhaps a relatively small number in the 3P state. Because the population in this category is such a large fraction of the total number of sodium atoms within the excitation volume, the percentage change in the population will be small at any given interval during the experiment. The second category will subsequently undergo substantial changes due to collisional relaxation processes and will become zero before the next repetition of the experiment. A rough knowledge of the magnitudes of the percentage changes in the populations of category I and category II sodium atoms in a given time interval proves to be important in the development of a theoretical description of the observed experimental results.

Category II can be divided into subcategories depending upon the subsequent fate of the atoms as equilibrium is reestablished in the cell following excitation. To category IIA we assign all Rydberg atoms that ionize (and then recombine) on their way back to the ground state. Category IIB includes all other Rydberg atoms, i.e. those which remain electrically neutral and eventually return to the ground state without ionizing.

How can category IIA atoms acquire the additional energy that they need in order to ionize? There are two possibilities: Collision (e.g., with a category I atom, another category II atom, with the walls or some other object within the cell, or with a free electron dislodged in a previous ionization process) or absorption or emission of a photon.

It seems likely that an insignificant fraction of the ionizations of category II atoms are caused by collisions with a category I atoms, because the latter are in their ground states. A ground state atom has no electronic energy available to transfer in a collision process, only relative translational kinetic energy, and these translational energies are typically too low at the temperatures of our experiments to ionize a 10D sodium atom.

Ionizing collisions with free electrons are possible, although such electrons are extracted from the excitation volume very rapidly via an electric field (typically 30V/cm) imposed upon the sample.

Collisions of Rydberg atoms with the electric field plates or with the walls cannot account for a significant fraction of the ionizations because this proess is too slow to deplete the category II population in the observed lifetimes.

Energy required for ionization cannot be easily acquired by the absorption of radiation either. Since the laser pulses have terminated, the only soures of photons in the cell are the luminescence of excited sodium atoms and the black - body radiation from the plates and surrounding cell walls (typically maintained at temperatures 10 or 20 degrees celsius above the oven temperature). Photons within this group having the correct frequencies to produce the necessary quantum transitions with high probability are scarce.

For all of these reasons, we believe that the dominant process responsible for ionization is the collision of one Rydberg with another. Even though the category II population constitutes only a small fraction of the total number of sodium atoms in the cell, the effective colisional cross-sections for Rydberg atoms are expected to be very large in comparison with those of ground state atoms. This enhanced size should more than compensate for the relatively small populations of such atoms, so that Rydberg - Rydberg collisions can play a very important role in determining the course of events after excitation.

A collision between two Rydberg atoms that does not lead directly to the ionization of one of them is irrelevant in assigning the colliding atoms to either of the two categories IIA and IIB. If the collision does lead to ionization, by definition one member of the colliding pair must be assigned to category IIA.

Due to the requirement of conservation of energy during the collision, the atom which does not ionize must lose energy. The loss of energy by an atom in its first collision implies a substantial decrease in the probability that it will be able to acquire sufficient energy to ionize in a subsequent collision. A Rydberg atom that does not ionize is by definition

assigned to category IIB. This means that an ionizing collision ordinarily assigns both of the colliding atoms to categories, one to IIA and the other to IIB.

Atoms which have not yet participated in ionizing collisions may eventually do so, and thus be assigned to categories IIA and IIB as described above. Competing with this collision process, however, are all of the other processes by means of which neutral atoms can return to the ground. If any category II atom loses energy by any of these processes before striking another category II atom, it will be unlikely to be able to acquire sufficient energy in the Rydberg - Rydberg collision process to be able to ionize. Such atoms will therefore also end up in category IIB.

To account for this, we create a new pair of subcategories. All Rydberg atoms assigned to category IIB by ionizing collisions will be assigned to cateory IIB#. All Rydberg atoms assigned to category IIB by processes other than Rydberg - Rydberg collisions will be assigned to category IIB*. The most important processes in the assignment of sodium atoms to category IIB* are likely to be unimolecular luminescence by Rydberg atoms (spontaneous emission) and collisions between Rydberg atoms and ground state atoms (category I - category II collisions).

It is appropriate here to note that the term "Rydberg" is more general than would be implied by the selectivity of the excitation process. A sodium atom initially produced in a particular Rydberg state (e.g., the 10D) can undergo transitions to other highly excited states differing from the first in either the l or the n quantum numbers (or both). These transitions are produced by collisions "softer" than those required for ionization, or by the absorption of radiation from sources described above (or both). Any such sodium atom would nevertheless be assigned to category II, and from II to the appropriate subcateory IIA, IIB#, or IIB*, depending upon its subsequent fate.

Thus we have grouped together, for convenience in the following analysis of the experimental data, excited sodium atoms whose paths back to the ground state may follow hundreds of different "decay channels". One further such experimental distinction is required. Of the many decay channels open to sodium atoms assigned to categories IIB# and IIB*, some of them will include a transition to the 4P state of neutral sodium, followed by a direct transition to the ground (3S) state by emission of a UV photon. Channels of decay which include these processes will be labelled + and channels which do not will be labelled -.

The significance of this distinction is that we monitored the light emitted from the sample cell with a photomultiplier tube preceded by interference filters which prevent any photons except those produced by the 4P -> 3S transition) oriented perpendicularly to the excitation axis from being detected.

To summarize, for any given laser shot, we assigned every sodium atom in the sample to one of the following categories:

I. Sodium atoms which are not excited to a Rydberg state.

II. Sodium atoms which are excited to a Rydberg state;

A. and which subsequently ionize,

B. or which never ionize.

Category IIB is further subdivided as follows:

IIB♯. Neutral Rydberg atoms which have ionized others by collision;

+. and return to the ground state by UV emission.

-. or which return without UV emission.

IIB*. Rydberg atoms which have never participated in an ionizing collision:

+. and return to the ground state by UV emission,

-. or which return without UV emission.

The signals which are digitized by the Biomation (both channels) are integrated on a Z80 - based microcomputer and stored on disc. Each integral from the first channel is proportional to the total number of electrons produced by ionization of sodium atoms in the sample following a single "shot" (pair of laser pulses). The corresponding integral from the second channel is proportional to the total number of UV photons produced by the sodium atoms in the sample due to the same "shot".

As was just mentioned, the transient voltage signals produced by the arrival of electrons at the positive plate inside the cell are fed to one channel of a Biomation transient digitizer, integrated by a Z80 - based microcomputer, and stored magnetically on a floppy disk. Any one of the resultant dimensionless numbers (i.e., in arbitrary units) EI, when multiplied by the appropriate scale factor ES, should be equal to the total number of electrons N(e) and therefore also equal to the number of sodium atoms that ended up in category IIA during that particular "shot". Let IIA be the total number of such atoms found at any instant of time in one unit of the active volume V. Then

$$N(e) = ES * EI = V * \int \langle IIA \rangle \, dt. \qquad (1)$$

The limits on this integral are 0 and infinity. Zero refers to the instant of time following laser excitation of the sample. Infinity refers to a time long after the bulk of the Rydberg atoms appear, but before an apreciable number of sodium ions have recombined with electrons to re-form ground state neutrals.

A similar treatment is given to the transient signals produced by the photomultiplier. They are fed to the other channel of the Biomation, integrated, and stored on disk. Any one of the resultant numbers PI, when multiplied by the appropriate scale factor PS, should be equal to the total number of photons N(p) and therefore also equal to the number of

sodium atoms that decay through channels that produce 4P 3S ultraviolet photons:

$$N(p) = PI * PS = V * \int (\langle IIB\#+\rangle + \langle IIB^{*}+\rangle)\ dt. \quad (2)$$

The limits on this integral are also 0 and infinity.

The problem is to develop a mathematical relationship between PE and PI that will allow the extraction of useful physical information about the decay processes of Rydberg atoms sodium from the experimental data.

First, we let R be the total Rydberg (category II) population density at any instant of time:

$$R = \langle IIA\rangle + \langle IIB\#+\rangle + \langle IIB\#-\rangle + \langle IIB^{*}+\rangle + \langle IIB^{*}-\rangle \quad (3)$$

It should be remembered that 'Rydberg' here does not refer solely to the state initially produced by the yellow and blue laser pulses, but also includes those closely related states differing from the original in the values of the n and l quantum numbers. R then might be called the population density in the 'Rydberg manifold'. Transitions to these states are produced from the original by low energy processes that have been discussed in previous paragraphs.

The equation that describes the time dependence of the Rydberg population is:

$$\frac{dR}{dt} = -k1 * R - k2 * R^2 \quad (4)$$

where t is the time and k1 and k2 are first and second order rate constants for unimolecular and bimolecular de-excitation, respectively. This equation deserves some comment, as it is to be considered *more* a symbolic representation of what is ultimately measured experimentally than it is a complete description of the dynamics of the depopulation of the Rydberg manifold. The first term on the rhs of Eq. 4 represents all of the decay channels for excited sodium atoms that we have placed in category IIB*. Therefore, we should have, for n channels:

$$k1 * R = k1(1) * R + k1(2) * R + \ldots + k1(n) * R \quad (5)$$

The terms on the rhs of Eq. 5 can be regrouped into those which give rise to a detectable UV photon (category IIB*+) and those which do not (category IIB*-):

$$k1 * R = \sum_{m=1,n} k1(m) * R \quad (6)$$

Cancel the R on both sides of Eq. 6 and then partition the sum on the rhs:

$$k1 = \sum_{m=1,j} k1(m) + \sum_{m=j+1,n} k1(m) \quad (7)$$

Rewrite each partial sum on the rhs of Eq. 7, using G to represent the fraction of IIB* atoms assigned to subcategory IIB*+ (and leaving 1-G to represent the fraction in subcategory IIB*-):

$$k1 = G * k1 + (1-G) * k1, \quad 0 < G < 1 \quad (8)$$

The second term on the rhs of Eq. 4 can be given a treatment similar to that given to the first term in Eqs. 5 - 8. The result is:

$$k2 = F * k2 + (1 - F) * k2, \quad 0 < F < 1 \tag{9}$$

Both terms on the rhs of Eq. 9 refer to bimolecular Rydberg - Rydberg collisions that assign one sodium atom to category IIA (thus producing an electron) and the other to category IIB#. The first term is associated with the fraction F of such collisions in which the unionized atom eventually produces a detectable UV photon and is thus assigned to subcategory IIB#+. The second term is associated with neutral atoms that return to the ground state without passing through the 4P level.

In addition to Eq. 4, we need rate equations that describe the production of electrons and photons. If we let the number of electrons produced per unit volume of the active region be Y:

$$dY/dt = k2' * R^2 \tag{10}$$

The integral of Eq. 10 is the desired expression in Eq. 1. Let the number of photons produced per unit volume of the active region be X:

$$\frac{dX}{dt} = G * k1' * R + F * k2' * R^2 \tag{11}$$

The integral of Eq. 11 is the desired expression in Eq. 2.

While the symbols used to represent the rate constants in Eq. 4 look similar to those employed in Eqs. 10 and 11, the primes in the latter equations are intended to call attention to an important distinction between them. Remember from Eqs. 6 and 7 that k1 and k2 are in reality composites made of many parallel decay channels. A further complication is the fact that each of these channels is ordinarily associated with a cascade of processes down the ladder of energy states from the Rydberg manifold to the ground state. Therefore, we cannot in general assign a single rate constant to the entire process. The complexity of the dynamics is easily seen from the pulse shapes recorded by the Biomation transient digitizer.

However, because we are attempting to fit only the integrals of the signals, we include automatically all decay channels that lead to the production of photons and electrons, regardless of the details. Thus it is appropriate to disregard these distinctions and interpret all rate constants as "effective" ones representing branching ratios more than actual relaxation times. Having said this, in what follows the primes will be dropped from the k's.

Equation 4 can easily be separated into expressions which depend only upon R and upon t:

$$\frac{dR}{k1 * R + 2 * k2 * R^2} = -dt \tag{12}$$

It is convenient to define:

$$K = 2 * \frac{k2}{k1} \tag{13}$$

Then:

$$dR/(R * (1 + K * R)) = \frac{dR}{R} - K * dR/(1 + (K * R)) \tag{14}$$

Equation 14 can be substituted into Eq. 12, and the resultant expression integrated from t = 0 to t = t

$$\ln \frac{R(t)}{R(0)} - \ln [(1 + K * R(t))/(1 + K * R(0))] = -k1 * t \tag{15}$$

Equation 15 can then be rearranged to yield:

$$(R(t) = A * \exp(-k1 * t)/(1 - K * A * \exp(-k1 * t)) \tag{16}$$

with:

$$A = \frac{R(0)}{1 - K * R(0)}. \tag{17}$$

By substituting:

$$Z = 1 - K * A * \exp - (k1 * t) \tag{18}$$

into Eq. 16, one can find:

$$I1 = \int R dt \tag{19}$$

and

$$I2 = \int R dt \tag{20}$$

I1 and I2 are just the integrals called for in Eqs. 1 and 2 (Eqs. 10 and 11):

$$ES * EI = V * k2 * I2 \tag{21}$$

and

$$PS * PI = V * ((G * k1 * I1) + (F * k2 * I2)) \tag{22}$$

The results of the two integrations in Eqs. 19 and 20 are:

$$k1 * K * I1 - \ln (1 + K * R(0)) \tag{23}$$

and:

$$k1 * K * I2 = R(0) + (k1 * I1) \tag{24}$$

Substitution of Eqs. 23 and 24 into Eqs. 21 and 22 yields:

$$2 * K * (\frac{ES}{V}) * EI = (K * R(0)) - \ln (1 + K * R(0)) \tag{25}$$

and:

$$2 * K * (\frac{PS}{V}) * PI = [(2 * G) - F] * \ln(1 + K * R(0)) + (F * K * R(0)) \tag{26}$$

In Eqs. 25 and 26, EI and PI are the experimental data stored on disk for the shot in question. The scale factors $\frac{PS}{V}$ and $\frac{ES}{V}$ are (in principle) measurable properties of the

experimental apparatus. The three quantities of physical interest are the branching ratios F and G, plus the ratio of rate constants K. Both experimental quantities are expressed parametrically in terms of R(0), the number of Rydberg atoms initially produced by the pair of laser pulses. It is the random variation in R(0) from shot to shot (due to frequency jitter in the lasers) that produces the observed variations in EI and PI, thus "scanning" the independent variable (normally taken to be PI).

We construct graphs to represent the data, with each point plotted on the graph representing a single shot. The y coordinate of each point is given by the measured EI and the x coordinate by the measured PI. Equations 25 and 26 implicitly specify a curve on this graph, which can be made to pass through the experimental points by the appropriate selection of F, G, and K. The best - fit values of these three quantities thus describe the results of any run, normally consisting of 1000 shots, associated with a particular temperature and a particular initial Rydberg state.

It is possible to combine Eqs. 25 and 26 by eliminating the common factor R(0) which appears therein. Alternatively, R(0) may be eliminated from either of them by means of the sum rule in Eq. 3. The successive terms on the rhs of that equation are equal to N(e), F * N(e), (1-F) * N(e), G * N(11B*), and (1-G) * N(11B*), respectively, where N(11B*) = $\int$ (<11B*+> + <11B*->) dt. Since the first and third terms add up to N(p), one can find a relationship among N(11B*), N(e) and N(p). This relationship can be substituted into Eq. 3 to yield:

$$N(p) = (G * R(0)) - ((2 * G) - F) * N(e) \qquad (27)$$

It is a simple matter to solve Eq. 27 for R(0) and substitute the result into either Eq. 25 or 26. However, the equation that results is still a transcendental one, so that the calculation of an explicit value of N(e) or EI from a given N(p) or PI is not entirely straightforward.

In fact, we found that were unable to obtain stable fits to the data unless the unknown scale factors ES/V and PS/V are fixed. Although the contract is over, a student is still working on this problem as part of his Ph.D. thesis. We have designed and built a small cell of known, measureable collection geometry so that measurements can now be made with known scale factors. This should enable us to determine the parameters F, G, and K. If the measurements are successful, a paper will be written describing the results.

References

1. R.L. Shoemaker, "Coherent transient effects in spectroscopy" in Annual Review of Physical Chemistry, Vol. 39, (1979).
2. R.L. Shoemaker in "Laser and Coherence Spectroscopy," J.I. Steinfeld, Ed., Plenum Press (1978), and references therein.
   R.G. Brewer in "Very High Resolution Spectroscopy," R.A. Smith, Ed., Academic Press (1976), and references therein.
3. N.A. Kurnit, I.D. Abella, and S.R. Hartmann, Phys. Rev. Letters, 13, 567 (1964).
4. R.L. Shoemaker and E.W. Van Stryland, J. Chem. Phys. 64, 1733 (1976).
5. R.G. Brewer and R.L. Shoemaker, Phys. Rev. A6, 2001 (1972).
6. R.G. Brewer and R.L. Shoemaker, Phys. Rev. Letters 27, 631 (1971).
7. P.R. Berman, J.M. Levy, and R.G. Brewer, Phys. Rev. A11, 1668 (1975).
8. R.L. Shoemaker, and F.A. Hopf, Phys. Rev. Letters 33, 1527 (1974).
9. Y. Prior and E.L. Hahn, Phys. Rev. Letters, 39, 1329 (1977).
10. M.M.T. Loy, Phys. Rev. Letters 32, 814 (1974).
11. R.L. Shoemaker and R.G. Brewer, Phys. Rev. Letters 28, 1430 (1972).
12. B. Boiger, and J.C. Diels, Physics Letters 28A, 401 (1968).
    P.F. Liao, J.E. Bjorkholm, and J.P. Gordon, Phys. Rev. Letters 39, 15 (1977).
    P.F. Liao, N.P. Economou, and R.R. Freeman, Phys. Rev. Letters 39, 1473 (1977).
    R.G. DeVoe and R.G. Brewer, Phys. Rev. Letters, 40, 862 (1978).
    R. Kachru, T.W. Mossberg, and S.R. Hartmann, Phys. Rev. A21, 1124 (1980), and references therein.
13. I.C. Percival in "Atoms and Molecules in Astrophysics," T.R. Carlson and M.J. Roberts, Eds., Academic Press (1972).
14. H. Figger, G. Leuchs, R. Straubinger, and H. Walther, Opt. Commun. 33, 37 (1980).
15. W.H. Wing, K.R. Lea, and W.E. Lamb, Jr., in Atomic Physics 3, edited by S.J. Smith and G.K. Walters (Plenum, New York, 1973), p. 119-141.
16. W.H. Wing and K.B. MacAdam, in Progress in Atomic Spectroscopy, edited by W. Hanle and H. Kleinpoppen (Plenum, New York, 1978).
17. W.E. Lamb, Jr., D.L. Mader, and W.H. Wing, in Fundamental and Applied Laser Physics, Proceeding of the Esfahan Symposium, edited by M.S. Feld, A. Javan, and N.A. Kurnit (Wiley, New York, 1973), pp. 523-538.
18. W.H. Wing and W.E. Lamb, Jr., Phys. Rev. Lett. 28, 265 (1972).
19. K.B. MacAdam and W.H. Wing, Phys. Rev. A12, 1464 (1975).
20. K.B. MacAdam and W.H. Wing, Phys. Rev. A13, 2163 (1976).
21. K.B. MacAdam and W.H. Wing, Phys. Rev. A15, 678 (1977).
22. M.G. Littman and H.J. Metcalf, Applied Optics 17, 2224 (1978).

I. Shoshan and U.P. Oppenheim, Optics Commun., 25, 375 (1978).

23. C. Freed, IEEE J. Quantum El. QE-4, 404 (1968).
24. K.C. Harvey and B.P. Stoicheff, Phys. Rev. Letters, 38, 537 (1977).
25. S.A. Lee, J. Helmcke, J.L. Hall, and B.P. Stoicheff, Optics Letters 3, 141 (1978).
26. S. Bashkin and J.O. Stoner Jr., "Atomic Energy level and Grotrian Diagrams," Vols. I and II, North-Holland, Amsterdam, 1976.
27. C. Freed, L.C. Bradley, and R.G. O'Donnell, IEEE J. Quantum El. QE-16, 1195 (1980).
28. J.W. Farley and W.H. Wing, Phys. Rev. A23, 2397 (1981).
29. M. Gross, C. Fabre, P. Pillet, and S. Haroche, Phys. Rev. Lett. 36, 1035 (1976).
    M. Gross, P. Goy, C. Fabre, S. Haroche, and J.M. Raimond, Phys. Rev. Lett. 43, 343 (1979).
30. J.M. Raimond, G. Vitrant, and S. Haroche, J. Phys. B, L655 (1981).